CYTOSKELETON

Vasohibins/SVBP are tubulin carboxypeptidases (TCPs) that regulate neuron differentiation

Chrystelle Aillaud,[1,2] Christophe Bosc,[1,2] Leticia Peris,[1,2] Anouk Bosson,[1,2] Pierre Heemeryck,[1,2] Juliette Van Dijk,[3,4] Julien Le Friec,[1,2] Benoit Boulan,[1,2] Frédérique Vossier,[1,2] Laura E. Sanman,[5] Salahuddin Syed,[5] Neri Amara,[5] Yohann Couté,[6] Laurence Lafanechère,[7] Eric Denarier,[1,2,8] Christian Delphin,[1,2] Laurent Pelletier,[1,2] Sandrine Humbert,[1,2] Matthew Bogyo,[5] Annie Andrieux,[1,2,8]*† Krzysztof Rogowski,[3]*† Marie-Jo Moutin[1,2]*

Reversible detyrosination of α-tubulin is crucial to microtubule dynamics and functions, and defects have been implicated in cancer, brain disorganization, and cardiomyopathies. The identity of the tubulin tyrosine carboxypeptidase (TCP) responsible for detyrosination has remained unclear. We used chemical proteomics with a potent irreversible inhibitor to show that the major brain TCP is a complex of vasohibin-1 (VASH1) with the small vasohibin binding protein (SVBP). VASH1 and its homolog VASH2, when complexed with SVBP, exhibited robust and specific Tyr/Phe carboxypeptidase activity on microtubules. Knockdown of vasohibins or SVBP and/or inhibitor addition in cultured neurons reduced detyrosinated α-tubulin levels and caused severe differentiation defects. Furthermore, knockdown of vasohibins disrupted neuronal migration in developing mouse neocortex. Thus, vasohibin/SVBP complexes represent long-sought TCP enzymes.

Microtubules are cytoskeletal polymers of α/β tubulin dimers centrally involved in cell division, motility, and morphogenesis. In the detyrosination/tyrosination cycle of tubulin, the C-terminal tyrosine of α-tubulin is removed by an elusive peptidase [tyrosine carboxypeptidase (TCP)] and re-added by the tubulin tyrosine ligase (TTL) (*1*). This cycle, which is specific to α-tubulin and mostly conserved from chordates to mammals, has a vital role in vivo (*2*). Tubulin detyrosination and tyrosination of α-tubulin is an important regulatory signal for mitosis (*3*–*5*), neuronal physiology (*6*–*8*), and muscle mechanotransduction (*9*, *10*). Consequently, abnormal tyrosination levels are associated with cell transformation and tumor aggressiveness (*11*, *12*), neuronal disorganization (*2*), and heart failure and cardiomyopathies (*10*, *13*). Although the detyrosination reaction was first described 40 years ago (*14*), the identity of TCP has remained unknown.

To enrich for TCP, we designed a three-step purification procedure using taxol-stabilized radiolabeled tyrosinated microtubules as a substrate to follow activity. A typical procedure gave a final purification factor of nearly 400-fold (Fig. 1A and fig. S1A). The last fraction (IV) was able to cleave the C-terminal tyrosine from tubulin incorporated in microtubules but not from EB1 (fig. S1B). EB1 is a protein that shares a similar C-terminal sequence with α-tubulin (-QEEY instead of -GEEY) and is generally not a substrate for TCP in physiological contexts (*15*).

To isolate the protein(s) responsible for TCP activity from fraction IV, we reasoned that an irreversible inhibitor could be used as in other chemical proteomic studies (*16*). We tested the sensitivity of brain TCP to various commercial protease inhibitors. The activity was inhibited by several serine/cysteine protease inhibitors [4-(2-aminoethyl)benzenesulfonyl fluoride hydrochloride (AEBSF), Tosyl-L-lysyl-chloromethyl ketone (TLCK), Tosyl phenylalanyl chloromethyl ketone (TPCK), E-64, and parthenolide] and by the thiol-reactive compound *N*-ethylmaleimide (Fig. 1B and fig. S2A). These results, in agreement with prior studies (*17*), strongly suggested that the catalytic activity of the putative TCP depends on a catalytic cysteine.

Although E-64 only showed modest inhibitory activity [median inhibitory concentration (IC_{50}) around 300 μM] (Fig. 1B), it is an ideal starting point for inhibitor design because its reactive epoxide electrophile can display a peptide- or amino acid–mimicking native protein C terminus. Furthermore, parthenolide, which is widely used to down-regulate detyrosination levels in cells (*4*, *6*, *9*, *10*), contains an epoxide function that is essential to its cellular effect (*17*). We thus synthesized three inhibitors—epoY, epoEY, and epoEEY—which contain the epoxide coupled to one, two, or three amino acids from the α-tubulin C terminus, respectively (fig. S2B). EpoY was the most potent inhibitor of the TCP activity (IC_{50} around 500 nM) (Fig. 1B). Alkyne-epoY, which retained a strong inhibitory potency (Fig. 1, B and C) and irreversibly inhibited the activity (fig. S2, C and D), was used to perform tetramethylrhodamine (TAMRA) labeling of fraction IV by means of click chemistry (Fig. 1D). This labeling showed specific modification of a small number of proteins (Fig. 1E). We then purified the inhibitor targets using agarose beads and, after on-beads trypsin digestion and quantitative mass spectrometry analyses of the resulting peptides from three independent experiments, we identified the protein vasohibin-1 (VASH1) as the most likely TCP candidate (Fig. 1D and tables S1 and S2). Peptides covering the almost full VASH1 sequence were detected (fig. S2E). Furthermore, recent bioinformatics data show that Vasohibin-1 and its homolog vasohibin-2 (VASH2) possess a noncanonical Cys-His-Ser catalytic triad and are members of the transglutaminase-like cysteine proteases family (Fig. 1F) (*18*).

Vasohibin proteins (41 to 42 kDa) have been extensively characterized as angiogenesis regulators but are poorly understood on a molecular level (*19*). Small vasohibin binding protein (SVBP) (Ccdc23) is a high-affinity binding partner of vasohibins that has a chaperone-like function (*20*). We examined the ability of VASH proteins to detyrosinate α-tubulin in cells in the absence or presence of SVBP. Expression of vasohibins alone in human embryonic kidney (HEK) 293T cells resulted in a slight increase of detyrosinated tubulin, whereas expression of either protein with SVBP resulted in a substantial increase in detyrosinated tubulin corresponding to a nearly complete loss of endogenous tyrosinated tubulin (Fig. 2A). Mutation of the putative catalytic cysteine on vasohibins [C179A for VASH1 and C158A for VASH2 (*18*)] abolished their capacity to produce detyrosinated tubulin. (Single-letter abbreviations for the amino acid residues are as follows: A, Ala; C, Cys; D, Asp; E, Glu; F, Phe; G, Gly; H, His; I, Ile; K, Lys; L, Leu; M, Met; N, Asn; P, Pro; Q, Gln; R, Arg; S, Ser; T, Thr; V, Val; W, Trp; and Y, Tyr. In the mutants, amino acids were substituted at certain locations; for example, C179A indicates that cysteine at position 179 was replaced by alanine.) Similarly, in mouse embryonic fibroblasts (MEFs), expression of the vasohibins with SVBP resulted in complete detyrosination of endogenous α-tubulin (Fig. 2B and fig. S3A).

α-Tubulins are generally encoded with a C-terminal tyrosine preceded by two glutamates.

[1]Grenoble Institut des Neurosciences (GIN), Université Grenoble Alpes, F-38000 Grenoble, France. [2]Inserm, U1216, F-38000 Grenoble, France. [3]Institut de Génétique Humaine (IGH), Université Montpellier, CNRS UMR9002, 34000 Montpellier, France. [4]Centre de Recherche en Biochimie Macromoléculaire (CRBM), Université Montpellier, CNRS UMR5237, 34000 Montpellier, France. [5]Department of Pathology, Stanford University School of Medicine, Stanford, CA 94305, USA. [6]Institut de Biosciences et Biotechnologies de Grenoble (BIG)–Laboratoire Biologie à Grande Échelle, Université Grenoble Alpes, CEA, INSERM, F-38000 Grenoble, France. [7]Team Regulation and Pharmacology of the Cytoskeleton, Institute for Advanced Biosciences, INSERM U 1209, CNRS UMR 5309, Université Grenoble Alpes, 38000 Grenoble, France. [8]BIG–Physiopathologie du Cytosquelette, CEA, F-38000 Grenoble, France.
*Corresponding author. Email: moutinm@univ-grenoble-alpes.fr (M.-J.M.); annie.andrieux@univ-grenoble-alpes.fr (A.A.); krzysztof.rogowski@igh.cnrs.fr (K.R.) †These authors contributed equally to this work.

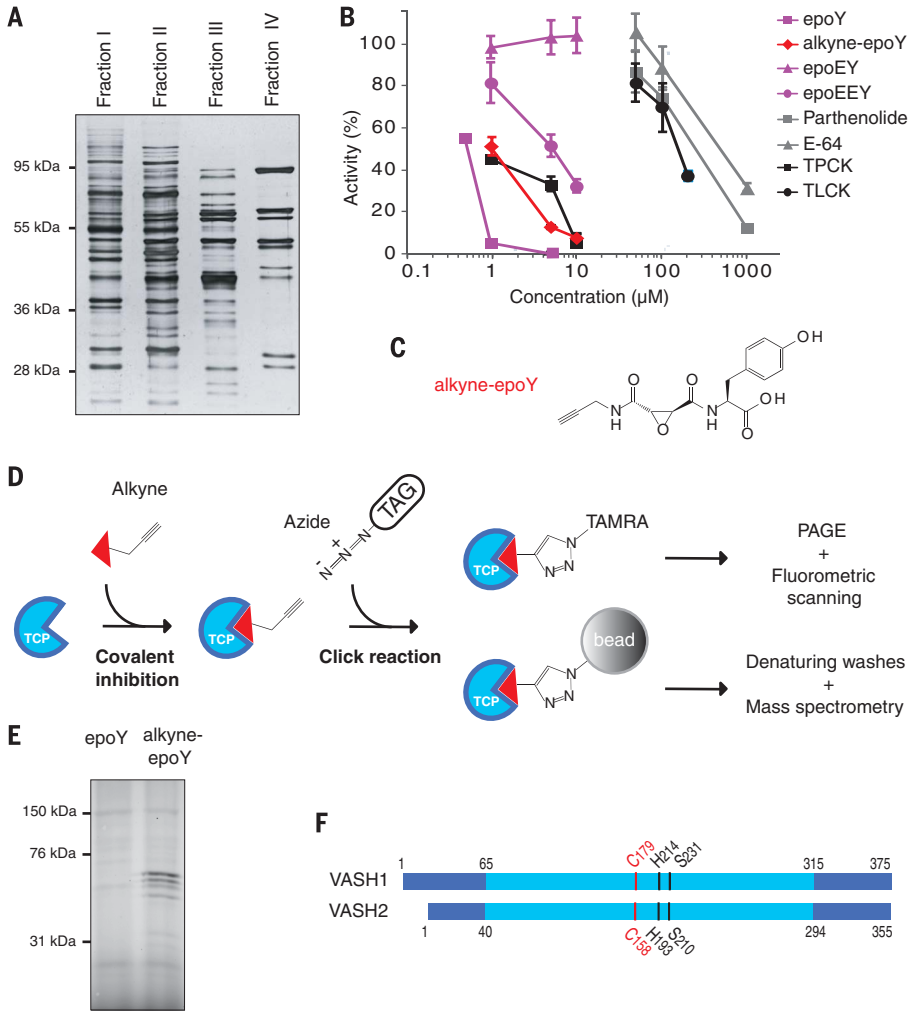

Fig. 1. Purification and identification of mouse brain TCP. (**A**) SDS–polyacrylamide gel electrophoresis (silver staining) of the indicated fractions of TCP enrichment from mouse brain (1 μg of proteins): ammonium sulfate precipitation step followed by two ion exchange columns stages (fig. S1A). (**B**) Fraction IV sensitivity to inhibitors. TPCK and TLCK are commercial serine/cysteine inhibitors containing either a Phe or a Lys residue. Fraction IV activity showed a 100-fold higher sensitivity to TPCK than to TLCK. E-64 is a natural product inhibitor of clan CA cysteine protease. EpoY, epoEY, and epoEEY are designed inhibitors containing an epoxide group coupled with Y, EY, or EEY amino acids, respectively. Alkyne-epoY is a clickable version of epoY. Results are expressed as percentage of enzyme activity (radioactivity assay) in the control with dimethyl sulfoxide (mean ± SD, n = 3 to 6 assays). (**C**) Structure of alkyne-epoY. (**D**) Schematic representation of the last steps of TCP identification by using Cu-catalyze azide-alkyne cycloaddition (click reaction). (**E**) Labeling of putative TCP from fraction IV with TAMRA red-fluorescent dye by using alkyne-epoY (nonclickable epoY is used as control). (**F**) Schematic representation of mouse vasohibin-1 and vasohibin-2 [69% overall sequence homology; 77% for core domains (clear blue boxes)]. These putative transglutaminase-like cysteine peptidases contain an unconventional triad of catalytic residues (Cys, His, and Ser).

α4-Tubulin lacks the C-terminal tyrosine, and α8-tubulin contains a C-terminal phenylalanine residue. Phenylalanine can be incorporated in place of tyrosine in tubulin and be a possible cause of neuronal dysfunction (*21*). We tested the substrate specificity of the vasohibins by overexpressing α1B- and α8-tubulin together with VASH1 or VASH2 and SVBP in HEK293T cells. Both tubulin isotypes were cleaved by active vasohibins when expressed with SVBP (Fig. 2C and fig. S3B). Vasohibins were unable to cleave the C-terminal residue when tyrosine was mutated to alanine (Fig. 2C and fig. S3B), confirming the specificity of VASH proteins for C-terminal tyrosine and phenylalanine residues.

We overexpressed vasohibins in HEK293T cells in the absence or presence of SVBP and purified the resulting complexes using a cobalt resin. SVBP copurified with both vasohibins as expected from previous affinity measurements [dissociation constant (K_d) 30 to 90 nM] (*20*), and complex formation was not dependent on catalytic activity (fig. S4A). The two protein complexes efficiently catalyzed tubulin detyrosination, whereas complexes containing the catalytic dead versions of the vasohibins were unable to detyrosinate tubulin (Fig. 2D). Both complexes cleaved microtubules more rapidly as compared with tubulin dimers (Fig. 2E and fig. S4B), which is consistent with the reported preference of brain TCP in in vitro experiments (*1*, *22*, *23*). Purified VASH1/SVBP complex was not able to cleave the C-terminal tyrosine from EB1, indicating its clear tubulin preference. Intriguingly, VASH2/SVBP complex was able to partially detyrosinate EB1 in the same conditions (Fig. 2F). In most cell types, including neuronal-derived cells, C-terminal tyrosine cleavage is restricted to tubulin (*1*, *15*). EB1 can, however, be detyrosinated in specific endothelial and tumor cells (*24*), and this may be related to their VASH2 contents or defect in a regulatory mechanism.

To confirm the functional importance of vasohibins and their role in α-tubulin detyrosination, we assessed the phenotypic effects of knocking down expression of these proteins in differentiating neurons, where the detyrosination/tyrosination cycle is highly important for growth cone pathfinding and axon differentiation—that is, for neuron polarization (*2*, *7*, *8*). Although we were unable to detect vasohibins and SVBP by means of immunoblot in mouse neurons using commercial antibodies, we amplified their transcripts from RNA preparations of cultured hippocampal neurons as well as of adult and embryonic mouse brain tissues (Fig. 3A and figs. S5A and S6A). We transfected hippocampal neurons with plasmids expressing short hairpin RNAs (shRNAs) targeting either the vasohibins or SVBP (validated in figs. S5B and S6B) as well as control shRNAs. The levels of detyrosinated α-tubulin were decreased by almost 50% when the two vasohibins, or the SVPB, were down-regulated. Addition of inhibitor (alkyne-epoY) also largely reduced detyrosinated α-tubulin (Fig. 3, B and C). When added together with the shRNAs, levels of detyrosinated tubulin were decreased up to 75% (Fig. 3, B and C). The remaining pool of detyrosinated α-tubulin could be due to incomplete depletion of vasohibins activities or to the presence of α4-tubulin, which genetically lacks the C-terminal tyrosine and remains in detyrosinated form in the brain (*25*). The occurrence of other detyrosinases can however not be excluded. Confocal images of neurons cultured 2 days in vitro (2DIV) confirmed a decrease in the levels of the native detyrosinated α-tubulin upon reduction of vasohibins expression or addition of inhibitor (Fig. 3D and fig. S5C). The remaining detyrosinated pools were specifically concentrated in the axon, whereas α-tubulin in the other neurites appeared

highly tyrosinated. Vasohibins down-regulation led to a clear delay in axonal differentiation (Fig. 3E). Tau and ankyrin G staining of neurons bearing an axon confirmed normal distribution, with Tau highly expressed in axon shaft at 3DIV and ankyrin G in the axon initial segment at 10DIV (fig. S7). Neurons 2DIV knocked down for vasohibins developed an increased number of neurites and branches with overall reduced axon length (Fig. 3F). A delay of axon differentiation and similar morphological anomalies were observed when down-regulating SVBP (fig. S6, D to F). Transfection of a plasmid allowing coexpression of shRNAs that target SVBP and a shRNA-resistant form of SVBP rescued α-tubulin detyrosination levels (fig. S6, A and C). Thus, contrary to the premature axonal differentiation observed in the absence of the reverse enzyme TTL (*2*), we observed a clear delay of axon differentiation when down-regulating vasohibins or SVBP.

We next tested the functional importance of vasohibins in vivo in mouse brain and focused on the cerebral cortex, where the detyrosination/tyrosination cycle is critical for the neocortex

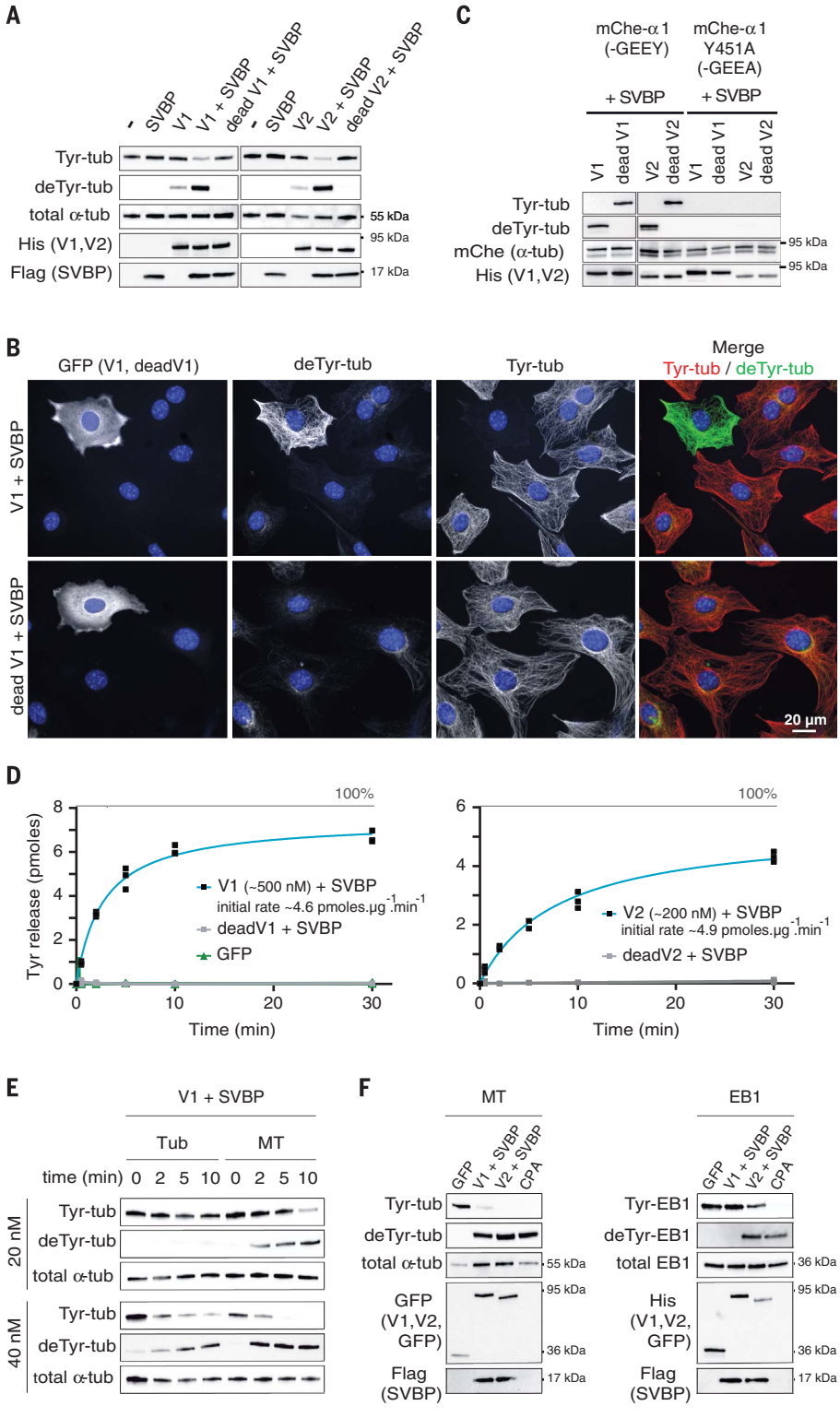

Fig. 2. Vasohibins associated to SVBP are potent tubulin tyrosine carboxypeptidases. (**A**) Immunoblot of endogenous tubulin from HEK293T cells expressing each VASH (V1 and V2) or their dead versions in the absence or presence of exogenous SVBP coexpression. Antibodies specific to tyrosinated and detyrosinated tubulin were used to assess detyrosination. Antibodies to α-tubulin, His, and Flag respectively reveal amounts of tubulin, vasohibin, and SVBP. Nontransfected cells (−) show endogenous levels of tubulin modifications. (**B**) Immunofluorescence images of detyrosinated/tyrosinated α-tubulin pools from MEF cells expressing active or inactive VASH1, and SVBP. Vasohibins were probed with antibody to green fluorescent protein (GFP). (**C**) Immunoblot of protein extracts from HEK293T cells expressing mCherry-α1B-tubulin, each VASH, and SVBP. Native or mutated versions of α1B-tubulin, respectively ending with EEY or EEA, were used. Levels of detyrosinated/tyrosinated tubulin were measured as in (A). Antibody to mCherry demonstrates same amounts of exogenous α-tubulin. (**D**) Detyrosination activity of purified VASH/SVBP complexes assessed by using [^{14}C]-tyrosinated taxol-stabilized microtubules (6 to 8 µM) (triplicate assay). Active and catalytic dead versions of the vasohibins were coexpressed with SVBP in HEK293T cells and purified on cobalt resin (fig. S4A). A purified GFP-His construct was used as a control. Data points were fitted with a single exponential (blue line). The theoretical maximal tyrosine release is indicated by a 100% line. (**E**) Detyrosination activity of purified VASH1/SVBP complexes (20 or 40 nM) on brain microtubules or tubulin dimers (5 µM) assessed by means of immunoblot. We controlled that tubulin was in dimeric or in assembled form (fig. S4C) and that the same amounts of enzymatic complexes were present (fig. S4D). (**F**) Detyrosination activity of purified VASH/SVBP complexes (600 nM) on brain microtubules or recombinant GFP-EB1 (5 µM). Enzyme quantities are much higher than in Fig. 2E. Carboxypeptidase A (CPA) was used as positive control. Antibodies against tyrosinated and detyrosinated EB1 were characterized in (*15*).

layer organization (2). During corticogenesis, neuronal migration relies in part on neuron polarization, which was highly dependent on vasohibins (Fig. 3, D and E) and SVBP (fig. S6, D and E). We electroporated embryonic day 14.5 (E14.5) embryos with the plasmids expressing shRNAs that target the vasohibins as well as control shRNA, and analyzed radial neuronal migration 4 days later. At E18.5, most neurons from control brains had reached the upper layer (bin 1), whereas when vasohibins were down-regulated, a significant fraction of neurons failed to do so (Fig. 4, A and B). Thus, these enzymes have a crucial role in neuronal migration during brain cortex development.

TCP remained the crucial missing element of the α-tubulin detyrosination/tyrosination cycle for 40 years. We identified vasohibins as enzymatic

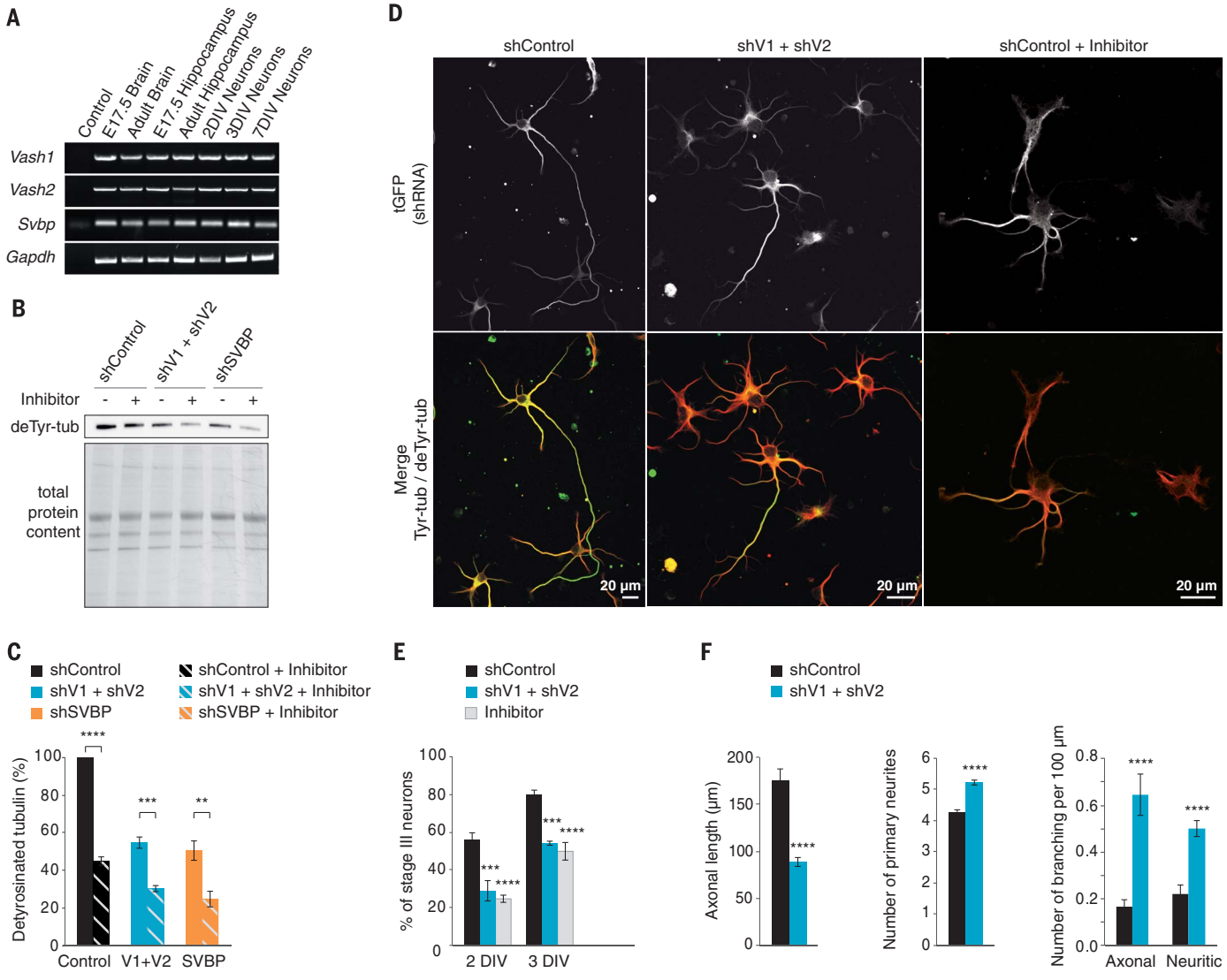

Fig. 3. Down-regulation of VASH1 and VASH2 affects neuronal differentiation. (**A**) *Vash1*, *Vash2*, and *Svbp* transcripts are found in brain tissues and hippocampal neurons. Reverse transcription polymerase chain reaction reactions of 45 cycles were performed, except for *Gapdh*, for which only 25 cycles were performed. (**B**) Immunoblot analysis of the effect of VASH1 and VASH2 (shV1+shV2) or SVBP (shSVBP) down-regulation with or without alkyne-epoY (inhibitor) on detyrosinated α-tubulin levels in neurons. Neurons were transfected by means of electroporation, with shRNAs associated to turboGFP (tGFP) cDNA just before plating and analyzed at 2DIV. Inhibitor (5 µM) was added at 0DIV and at 1DIV. Results are from duplicate immunoblots of three independent neuronal cultures. (**C**) Quantification of immunoblots as in (B) (duplicate of four to eight independent neuronal cultures). Results are expressed as percentage of detyrosinated tubulin related to shControl (mean ± SEM). Detyrosinated tubulin was significantly reduced in all conditions compared with shControl [one-way analysis of variance (ANOVA) with Sidak's multiple comparisons test]. Detyrosinated tubulin was additionally reduced when shV1+shV2 and shSVBP transfected neurons were incubated with the inhibitor (Student's *t* test). (**D** to **F**) Effect of vasohibins down-regulation on neurite outgrowth and axonal differentiation. Neurons were transfected as in (B) and analyzed by means of immunostaining at 2DIV and 3DIV. (D) Tyrosinated and detyrosinated α-tubulin levels were imaged at 2DIV using the same antibodies as in Fig. 2A. Levels of shRNA were imaged by using an antibody to tGFP. The size of scale bars are different. (E) Stage III neurons (bearing an axon) were counted manually on immunofluorescence images [generated as in (C)] from 4 to 10 independent cultures, at 2DIV and 3DIV. Proportion of stage III neurons (an index of neuronal differentiation) is represented as mean ± SEM (one-way ANOVA with Bonferroni multiple comparison test). (F) Morphometric analyses of at least 85 neurons (2DIV) by using AutoNeuriteJ macro (details are available in the supplementary materials, materials and methods) on immunofluorescence images generated as in (D) (mean ± SEM, Mann-Whitney tests). In (C), (E), and (F): $*P < 0.05$, $**P < 0.01$, $***P < 0.001$, $****P < 0.0001$.

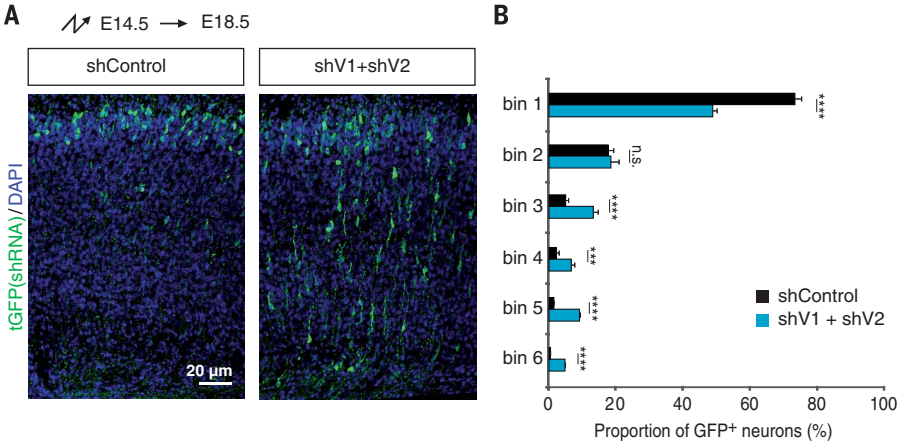

Fig. 4. Down-regulation of vasohibins affects radial migration of newborn cortical neurons. (**A**) Cortical coronal sections of E18.5 mice embryos electropored at E14.5 with indicated shRNAs. (**B**) Quantitative analysis showing the distribution of tGFP-positive neurons across the cortex divided into six bins of equal surface. Data are from five brains per condition, three slides per embryo (at least 260 GFP^+-neurons per embryo), mean ± SEM. n.s., not significant; ***$P < 0.001$, ****<0.0001 (Mann-Whitney test).

proteins that perform the TCP function (fig. S8). The failure of prior attempts to identify TCPs most probably resulted from their association with SVBP for stability and activity, which could likely be lost during standard purification assays. In agreement with TCP functions, vasohibins are widely distributed in eukaryotes and have broad tissue expression, and vasohibin-1 (which is generally more expressed than vasohibin-2) is abundant in the brain, heart, and kidney [(*18*, *26*, *27*) and GTEx Portal, on www.gtexportal.org/home]. Additionally, we demonstrated their critical role in neuron and brain physiology.

REFERENCES AND NOTES

1. H. S. Barra, C. A. Arce, C. E. Argaraña, *Mol. Neurobiol.* **2**, 133–153 (1988).
2. C. Erck *et al.*, *Proc. Natl. Acad. Sci. U.S.A.* **102**, 7853–7858 (2005).
3. A. C. Badin-Larçon *et al.*, *Proc. Natl. Acad. Sci. U.S.A.* **101**, 5577–5582 (2004).
4. M. Barisic *et al.*, *Science* **348**, 799–803 (2015).
5. L. Peris *et al.*, *J. Cell Biol.* **174**, 839–849 (2006).
6. P. Gobrecht *et al.*, *J. Neurosci.* **36**, 3890–3902 (2016).
7. Y. Konishi, M. Setou, *Nat. Neurosci.* **12**, 559–567 (2009).
8. S. Marcos *et al.*, *PLOS ONE* **4**, e5405 (2009).
9. J. P. Kerr *et al.*, *Nat. Commun.* **6**, 8526 (2015).
10. P. Robison *et al.*, *Science* **352**, aaf0659 (2016).
11. L. Lafanechère *et al.*, *J. Cell Sci.* **111**, 171–181 (1998).
12. R. A. Whipple *et al.*, *Cancer Res.* **70**, 8127–8137 (2010).
13. S. Belmadani, C. Poüs, R. Ventura-Clapier, R. Fischmeister, P. F. Méry, *Mol. Cell. Biochem.* **237**, 39–46 (2002).
14. M. E. Hallak, J. A. Rodriguez, H. S. Barra, R. Caputto, *FEBS Lett.* **73**, 147–150 (1977).
15. A. Bosson *et al.*, *PLOS ONE* **7**, e33490 (2012).
16. M. A. Child *et al.*, *Nat. Chem. Biol.* **9**, 651–656 (2013).
17. X. Fonrose *et al.*, *Cancer Res.* **67**, 3371–3378 (2007).
18. L. Sanchez-Pulido, C. P. Ponting, *Bioinformatics* **32**, 1441–1445 (2016).
19. Y. Sato, *J. Biochem.* **153**, 5–11 (2013).
20. Y. Suzuki *et al.*, *J. Cell Sci.* **123**, 3094–3101 (2010).
21. Y. Ditamo, Y. M. Dentesano, S. A. Purro, C. A. Arce, C. G. Bisig, *Sci. Rep.* **6**, 38140 (2016).
22. G. G. Deanin, S. F. Preston, R. K. Hanson, M. W. Gordon, *Eur. J. Biochem.* **109**, 207–216 (1980).
23. N. Kumar, M. Flavin, *J. Biol. Chem.* **256**, 7678–7686 (1981).
24. A. Rovini *et al.*, *PLOS ONE* **8**, e65694 (2013).
25. V. Redeker, *Methods Cell Biol.* **95**, 77–103 (2010).
26. S. Nimmagadda *et al.*, *Dev. Dyn.* **236**, 1358–1362 (2007).
27. T. Shibuya *et al.*, *Arterioscler. Thromb. Vasc. Biol.* **26**, 1051–1057 (2006).

ACKNOWLEDGMENTS

We dedicate this manuscript to Dr. Hector Barra, father of the detyrosination/tyrosination cycle who passed away on 2 December 2016. We are grateful to D. Job who strongly supported initiation of the project and for his constant encouragement. We thank M. Comte, E. Martin, C. Corrao, and C. Paoli for technical assistance. We thank members of the Plateforme d'Imagerie Cellulaire du Grenoble Institut des Neurosciences for their help in cell imaging and zootechnicians of the Grenoble Institut des Neurosciences for animal care. We thank M. Steinmetz for providing purified TTL and A. Beghin for initial development of AutoNeuriteJ macro. We thank the support of the discovery platform and informatics group at EDyP. This work was supported by INSERM, CEA, Université Grenoble Alpes, CNRS, and by La Ligue Contre le Cancer comités de l'Isère et de Savoie (to M.-J.M.), Association pour la Recherche sur le Cancer (grants SFI20111204053 to M.-J.M., DOC20120605000 to A.B., and 20151203348 to L.L.), Fondation pour la Recherche Médicale grant FDT20160435356 (to C.A.), Agence National de la Recherche grant ANR-13-JSV2-0002/TYRTUB (to K.R.), Institut National du Cancer grant 2016-165 (to LL) and the National Institutes of Health grant R01 EB005011 (to M.B.). Proteomic experiments were partly supported by the ProFi grant (ANR-10-INBS-08-01). An EU patent titled "Methods and pharmaceutical compositions for treating tubulin carboxypeptidases associated diseases" has been filed by Inserm and UGA (patent application no. EP17306476.7). Data described can be found in the main figures, supplementary materials, and table S2.

SUPPLEMENTARY MATERIALS

www.sciencemag.org/content/358/6369/1448/suppl/DC1
Materials and Methods
Supplemenatry Text
Figs. S1 to S7
Tables S1 and S2
References (*28*–*37*)

27 July 2017; accepted 3 November 2017
Published online 16 November 2017
10.1126/science.aao4165

Science

Vasohibins/SVBP are tubulin carboxypeptidases (TCPs) that regulate neuron differentiation

Chrystelle Aillaud, Christophe Bosc, Leticia Peris, Anouk Bosson, Pierre Heemeryck, Juliette Van Dijk, Julien Le Friec, Benoit Boulan, Frédérique Vossier, Laura E. Sanman, Salahuddin Syed, Neri Amara, Yohann Couté, Laurence Lafanechère, Eric Denarier, Christian Delphin, Laurent Pelletier, Sandrine Humbert, Matthew Bogyo, Annie Andrieux, Krzysztof Rogowski and Marie-Jo Moutin

Science **358** (6369), 1448-1453.
DOI: 10.1126/science.aao4165originally published online November 16, 2017

Tubulin carboxypeptidase identity revealed

Enzymes of the α-tubulin detyrosination/tyrosination cycle create landmarks on microtubules that are essential for their multiple cellular functions and are altered in disease. Tubulin carboxypeptidases (TCPs) responsible for detyrosination have remained elusive for 40 years (see the Perspective by Akhmanova and Maiato). Aillaud *et al.* identified vasohibins as enzymes that perform the TCP function and found that their small interacting partner SBVP was essential for their activity. Vasohibin/SVBP complexes were involved in neuron polarization and brain cortex development. The authors also developed an inhibitor targeting this family of enzymes. Using a completely different strategy, Nieuwenhuis *et al.* also showed that vasohibins can remove the C-terminal tyrosine of α-tubulin.

Science, this issue p. 1448, p. 1453; see also p. 1381